COMMUNICATIONS IN SCIENCE AND TECHNOLOGY
Homepage: cst.kipmi.or.id

Study in the impact of quaternized graphene oxide (QGO) composition as modifier on the chemical, physical, mechanical, and performance properties of polyvinylidene fluoride (PVDF)-based nanocomposite membrane

Ashabul Kahfi[a], Nita Kusumawati[a,*], Pirim Setiarso[a], Supari Muslim[b], Sinta Anjas Cahyani[a], Nafisatus Zakiyah[a],

[a]*Department of Chemistry, Universitas Negeri Surabaya, Surabaya 60231, Indonesia.*
[b]*Department of Electrical Engineering, Universitas Negeri Surabaya, Surabaya 60231, Indonesia.*

Article history:
Received: 13 February 2024 / Received in revised form: 16 May 2024 / Accepted: 16 May 2024

Abstract

Polyvinylidene Fluoride (PVDF) membranes were modified with quaternized graphene oxide (QGO) synthesized from graphene oxide and quaternized ammonium groups. PVDF/QGO membranes were created by blending PVDF and 0.01-0.05 g QGO via phase inversion. FTIR confirmed the successful QGO incorporation. PVDF/QGO membranes exhibited increased mechanical stiffness. Meanwhile, SEM revealed asymmetric morphology with surface and internal pores. AFM showed the membrane with 0.05 g and QGO had the highest surface roughness of 101.2 nm, which increased filtration area and flux. QGO improved hydrophilicity through hydroxyl and quaternary ammonium groups, enhancing water flux up to 1208 $Lm^{-2}h^{-1}$ for 0.05 g QGO. Cu^{2+} rejection increased to 75% for 0.05 g QGO membrane due to chelation and adsorption effects. PVDF/QGO membranes displayed bacterial growth inhibition, unlike pristine PVDF. The inhibition zone diameter increased with more QGO, indicating improved antibacterial activity. Overall, this study demonstrated that QGO improved PVDF membranes' hydrophilicity, antibacterial properties, and mechanical strength.

Keywords: Polyvinylidene fluoride; graphene oxide; quaternary ammonium; hydrophilicity; antibacterial

1. Introduction

Membrane separation is an effective and environmentally friendly technique to eliminate any phenolic compounds from industrial wastewater, lowering health hazards and environmental consequences [1]. Biofouling poses a major obstacle to the practical application of membrane technology for separation processes. The formation of biofilm on membrane surfaces enables microorganisms and bacteria to adhere and proliferate, consequently reducing membrane flux and lifespan [2]. Regular physical or chemical cleaning to control biofouling leads to high operational and maintenance expenses. Moreover, such cleaning practices may permanently damage the membrane. An effective strategy to mitigate biological contamination of membranes involves modifying the membrane materials to impart antibacterial properties [3].

By introducing hydrophilic modifications to the membrane, its surface becomes capable of forming a hydrated layer that effectively isolates proteins, bacteria, and other contaminants [4]. This modification makes the material more hydrophilic, decreasing hydrophobic interactions and allowing microorganisms to adhere to it. However, even though the material is now more hydrophilic, it lacks the ability to kill bacteria that are able to initially attach to the membrane surface before the modification is made.

Consequently, deposited bacteria can still thrive and form biofilms on the membrane surface [5]. On the other hand, membranes endowed with antibacterial characteristics can efficiently eradicate bacteria present on the membrane surface, thereby thwarting the development of biofilms. Nevertheless, Intra-cellular substances like proteins originating from deceased bacteria might reattach to the membrane surface, especially in cases where the membrane displays hydrophobic properties. Therefore, membrane modification with dual hydrophilic and antibacterial properties is considered as an ideal method to address membrane biofouling, representing a primary focus in current membrane modification research [6,7,8,9].

Numerous investigations have suggested different

* Corresponding author.
Email: nitakusumawati@unesa.ac.id
https://doi.org/10.21924/cst.9.1.2024.1393

innovative methods for dual-purpose membrane enhancement. For instance, a study presented a membrane coated with a zwitterionic polymer brush by immobilizing catechol on the surface of the membrane [10]. The zwitterionic-modified membrane demonstrated the improved hydrophilicity and antibacterial characteristics, leading to a notable reduction in protein and bacterial adhesion. On the other hand, modifications to a polyethersulfone membrane using post-ultraviolet irradiation treatment with a zwitterionic polyampholyte hydrogel, followed by graphene oxide filling applied [11] showed a noticeable enhancement of the modified membrane's hydrophilicity and antibacterial characteristics. However, post-membrane treatment and the complex zwitterion process could potentially damage the membrane material. Membrane modification through modifier blending, therefore, becomes a more convenient option although the challenge lies in obtaining modifiers with dual hydrophilic and antibacterial functions without experiencing loss from the modified membrane.

Graphene oxide (GO) demonstrates promising characteristics for enhancing membrane properties. The abundant hydroxyl groups present in graphene oxide, coupled with its exceptional hydrophilicity, render it an ideal candidate for such applications. Furthermore, the irregular sheet structure of graphene oxide can easily be trapped in the polymer membrane material during the process of converting the casting solution from a liquid to a solid phase [12]. This results in a hydrophobic carbon framework trapped within the membrane, enriched with hydrophilic groups at the membrane-water interface. Moreover, the presence of carboxyl and epoxy groups on GO provides opportunities to attach various functional groups with specific functions, making it a highly flexible modifier for membrane modification [13]. While reports suggest that GO may exhibit certain antibacterial properties; its success in achieving significant antibacterial properties in modified membranes has not been fully established [14]. Hence, this study aims to utilize graphene oxide (GO) as a carrier for incorporating antimicrobial agents as modifiers to enhance both the water-attracting and antibacterial characteristics of the membrane.

Quaternary ammonium groups are recognized for their potent antimicrobial attributes, largely attributed to their elevated positive charge concentration and efficient electrostatic interactions having negatively charged cellular membranes. Alkane chains in these groups can also penetrate bacterial cells, resulting in bacterial inactivation. Although water-soluble quaternary ammonium has been proven to be capable of enhancing hydrophilic and antimicrobial properties, the challenge lies in controlling the loss of this additive from the modified membrane [15].

In this study, epoxy and carboxyl groups present on graphene oxide were employed as reactive sites for covalently attaching quaternary ammonium groups, resulting in the production of quaternized graphene oxide (QGO) with dual hydrophilic and antibacterial traits characteristics. Subsequently, QGO was utilized as a modifying agent during the manufacturing process of QGO-PVDF membranes employing the phase inversion technique. Ultimately, the novel QGO-PVDF membrane, which exhibited both hydrophilic and antibacterial properties, was successfully manufactured and comprehensively characterized. Unlike other methods, the blending method involving QGO enables the fabrication of membranes and surface alteration with dual functionality in a single process, making it more practical and competitive for industrial applications.

2. Materials and Methods

2.1. Materials

PVDF powder (Molecular weight ~534,000), N, N-Dimethylacetamide (DMAc, purity 99%), acetone (purity 99.5%), dimethyloctadecyl [3 (Trimethoxysilyl)propyl]ammonium chloride (DMOAP), and toluene (purity 99.8%) were procured from Sigma Aldrich, Singapore. Hydrochloric acid (HCl, concentration 37%), hydrogen peroxide (H_2O_2, concentration 30%), ethanol (concentration 96%), sodium nitrate ($NaNO_3$, powder), sulfuric acid (H_2SO_4, concentration 98%), potassium permanganate ($KMnO_4$), $CuSO_4$, NaOH, and Na_2CO_3 were obtained from PT. Smartlab Indonesia, Indonesia. Graphite powder was purchased from Merck, Germany, while distilled water was acquired from CV. Chemical Indonesia Multi Sentosa, Indonesia.

2.2. Method

2.2.1. Graphene oxide (GO) preparation

GO was synthesized by adapting the procedure initially proposed by Hummers and Offerman. In detail, 10 g of graphite powder and 5 grams of $NaNO_3$ were combined in 230 mL of cooled sulfuric acid with gradual stirring at 10°C. Following this, 30 grams of $KMnO_4$ was introduced, and the mixture underwent heating and stirring at 35°C for 30 minutes. Following the addition of 250 mL of distilled water, the temperature was raised to 90°C, and stirring persisted for an additional 30 minutes at this elevated temperature. To cease the oxidation process, 500 mL of distilled water and 50 mL of a H_2O_2 30% solution were sequentially added to reduce excess $KMnO_4$. Following this, the resulting sample was centrifuged at 8000 rpm for 10 minutes and dried in a vacuum oven at 60°C for 24 hours.

Table 1. Compositions of QGO-PVDF solutions

Membrane	PVDF (gram)	DMAc (gram)	Acetone (gram)	QGO (gram)
Q0	2.7	9	6	0
Q1	2.7	9	6	0.01
Q2	2.7	9	6	0.02
Q3	2.7	9	6	0.03
Q4	2.7	9	6	0.04
Q5	2.7	9	6	0.05

2.2.2. Quaternized graphene oxide (QGO) synthesis

The preparation of Q-GO was conducted by following the procedure described by Changkhamchom et al. [16]. Initially, 0.1 grams of GO powder were dispersed in 50 milliliters of

toluene through sonication for 2 hours. Subsequently, 5 grams of DMAOP were introduced to the GO suspension at a temperature of 27°C and stirred for 36 hours. The resulting product underwent centrifugation and was washed four times with 100 milliliters of ethanol to eliminate toluene and any unreacted DMAOP molecules. Finally, the resulting product was subjected to drying at 55°C for a duration of 24 hours to yield the QGO powdered form.

2.2.3. Membrane preparation

The QGO-PVDF membrane was produced through a phase separation method employing an electrospinning casting technique. The membrane was produced by combining PVDF powder (18%) in a solution of DMAc and acetone ratio (3:2) as the matrix polymer. Different amounts of QGO (0.01; 0.02; 0.03; 0.04; and 0.05 grams) were utilized as the additional components to produce a range of QGO-PVDF composite membranes (refer to Table 1). The blend was agitated for 12 hours at 65°C with a stirring rate of 270 rpm. Electrospinning casting was carried out for 2 hours, applying a voltage of 15 kV, flow velocity of 1 mL/hour, and maintaining a separation distance of 15 cm between the injector and the collector drum, as outlined in the study conducted by Kusumawati et al. [17].

2.3. Membrane characterization

The QGO-PVDF membrane's chemical properties were validated through PerkinElmer Fourier Transform Infrared (FTIR) Spectrum Two. To assess the membrane's mechanical characteristics, RCT-10KN-AF Toyo Seiki Strograph was employed. The morphology of both the surface and cross-sections of the membranes was examined using the FEI Inspect S50 Scanning Electron Microscope (SEM). For measuring membrane permeability, a "dead-end" (self-made) membrane reactor was utilized, and the resulting permeate's selectivity was analyzed with AA-7000 Shimadzu Atomic Absorption Spectrophotometry (AAS). The membrane physical characterization involved the analysis of the surface roughness of the most optimal membrane using Bruker Atomic Force Microscopy (AFM).

2.4. Membrane porosity analysis

Porosity analysis was conducted by examining scanning electron microscope (SEM) images using OriginPro 2018 software. Here, the parameters needed included the maximum and minimum height values (Hmax, Hmin), x and y dimensions, integral volume, total volume, solid volume, volume under the curve, pore volume, and porosity percentage. The software calculated porosity percentage using the following equation:

$$V_{solid} = \int_{x_{min}}^{x_{max}} \int_{y_{min}}^{y_{max}} f\,(x,y)dxdy \quad (1)$$

where X_{max}, X_{min}, Y_{max}, Y_{min} are the surface boundaries at X and Y coordinates (surface boundaries when projected on the base plane), equation 2 to find the total volume,

$$V_{total} = f_{max}\,(x_{max} - x_{min})(y_{max} - y_{min}) \quad (2)$$

The difference of total volume and solid volume was to find the pore volume, and equation 3 was to find porosity and its percentage,

$$\phi = \frac{V_p}{V_{tot}} \quad (3)$$

where ϕ is porosity, V_p is pore volume, and V_{tot} is total volume.

2.5. Membrane performance evaluation

The QGO-PVDF membrane's permeability and selectivity were determined using Equations (4) and (5) as follows:

$$J = \frac{V}{A \times t} \quad (4)$$

$$R = \left(1 - \frac{C_p}{C_f}\right) \times 100\% \quad (5)$$

In this context, J represents the pure water flux (measured in $Lm^{-2}h^{-1}$), V denotes the volume of permeation (measured in L), A indicates the membrane's effectiveness area (measured in m^2), t signifies the filtration time (measured in hours), R expresses the removal ratio of Cu^{2+} (in percentage), and C_f and C_p denote the levels of Cu^{2+} in the feed and filtrate, respectively.

2.6. Bacteria inhibition test

The effectiveness of the QGO-PVDF membrane against bacteria was assessed using the agar disk diffusion method. For this approach, the bacteria with a Gram-negative cell wall E. coli was chosen as the reference organism, and all procedures were conducted under sterile conditions. Before being cultured on Mueller-Hinton agar plates, each bacterial sample was introduced into a suspension with approximately 1.5 × 108 cfu/ml colonies. A 12 mm-diameter segment of the QGO-PVDF membrane was then placed in an incubator at 37°C for 24 hours. The resulting membrane was then assessed for the presence of an inhibition zone three times using a calliper. The antibacterial efficacy of the membranes was assessed by examining the presence of a zone of inhibition surrounding each membrane, following the method as outlined by Xu et al. [20].

3. Results and Discussion

3.1. Chemical properties analysis with FTIR

Fig. 1 illustrates the FTIR spectra of QGO-PVDF membranes (Q0-Q5). The pristine PVDF membrane (Q0) displayed peaks at 1401.51 cm^{-1} associated with C-H stretching and deformation vibrations, a peak at 1171.32 cm^{-1} representing C-F groups, and a peak at 876.07 cm^{-1} as a characteristic feature of the PVDF β phase [21,22]. These peaks were also observed for Q1-Q5. The IR spectra of Q1-Q5 membranes displayed a signature peak ranging from 2959.49 to 3020.36 cm^{-1}, denoting the existence of O-H groups intrinsic to QGO. Specifically, the emergence of a peak at 1732.84 cm^{-1} (C=O) reinforced the incorporation of GO in the composite membranes, further validated by the transmittance percentages.

The systematic interpretation of the spectra suggests the successful fabrication of the QGO-PVDF composite membranes. The optimal variation was attained at Q5 composition with the highest GO loading across the variants.

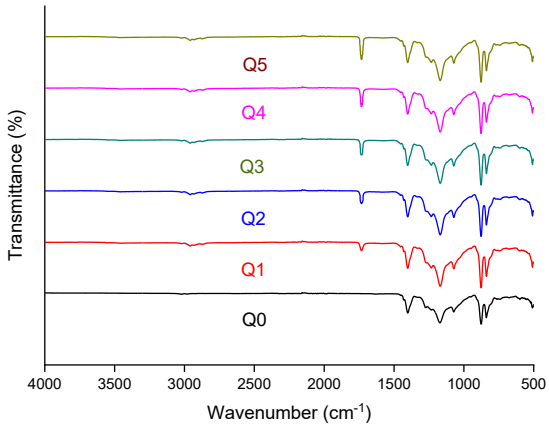

Fig. 1. FTIR results of QGO-PVDF membrane

3.2. Mechanical strength analysis

The mechanical durability of the QGO-PVDF membranes was evaluated by determining Young's modulus, computed by dividing the applied load by the resulting deflection, following Equation 6 as detailed in the study.

$$E = \frac{Stress}{Strain} \quad (6)$$

Table 2. Modulus young membrane QGO-PVDF

Membrane	PVDF (gram)	QGO (gram)	Modulus Young (Mpa)
Q0	2.7	0	8.40
Q1	2.7	0.01	13.93
Q2	2.7	0.02	14.65
Q3	2.7	0.03	15.32
Q4	2.7	0.04	15.45
Q5	2.7	0.05	15,62

Young's modulus represents the stress-to-strain relationship with the elastic limit of a material. A higher Young's modulus indicates greater stiffness and ability to withstand deformation under stress. Table 2 shows that Q2-Q5 had a monotonic increase in Young's modulus as the mass fraction of QGO increased in the PVDF matrix. This was determined by the closer packing of molecules in the QGO/PVDF composite membranes having created a more stable framework [23]. Numerous functional groups present on QGO contributed to improved interactions at the interfaces, facilitating the transfer of polymer to QGO and influencing the van der Waals forces between the layers. These attributes aided in the easy dispersion of QGO within the polymer matrix. Previous studies confirmed the outstanding compatibility between GO and the PVDF polymer matrix at the interface [24]. This is in agreement with composite theory where inorganic fillers tend to increase the stiffness of composite materials. This statement is supported by Alasfar et al. [25] stating that the addition of inorganic particles into a polymer would result in an increase in elastic modulus or Young's modulus. Also, Essabir et al. [24] stated that the addition of inorganic particles into a polymer would result in the interaction between PVDF chains with inorganic graphene oxide filler causing an increase in the stiffness of the polymer matrix and an increase in elastic modulus or Young's modulus. Thus, the addition of QGO has significantly increased the mechanical stiffness of the PVDF membrane through the mechanism of particulate reinforcement.

3.3. Membrane morphology analysis.

Fig. 2 displays the surface morphology and cross-sectional views of the QGO-PVDF composite membrane system. As the amount of QGO added increased, a reduction in pore size was observed, particularly evident with the addition of 0.03 g (Q3) and 0.05 g (Q5) of QGO, as depicted in Fig. 2 (a-c). Fig. 2 (d-f) illustrate that the PVDF membrane (Q0), QGO-PVDF membrane (Q3), and QGO-PVDF membrane (Q5) exhibited typical asymmetric structures, comprising a surface layer, finger-shaped pores, and sponge-shaped pores layer at the bottom. The addition of QGO led to an enhancement in membrane hydrophilicity, consequently improving the spreading or dispersal rates of organic solvents as well as water and resulting in accelerated membrane densification. However, the increased mass of QGO also elevated the solution viscosity, impeding the diffusion of organic solvents and water within the membrane and reducing the phase change rate. Consequently, the sponge-shaped pores of the membrane were substantially enlarged [26,27].

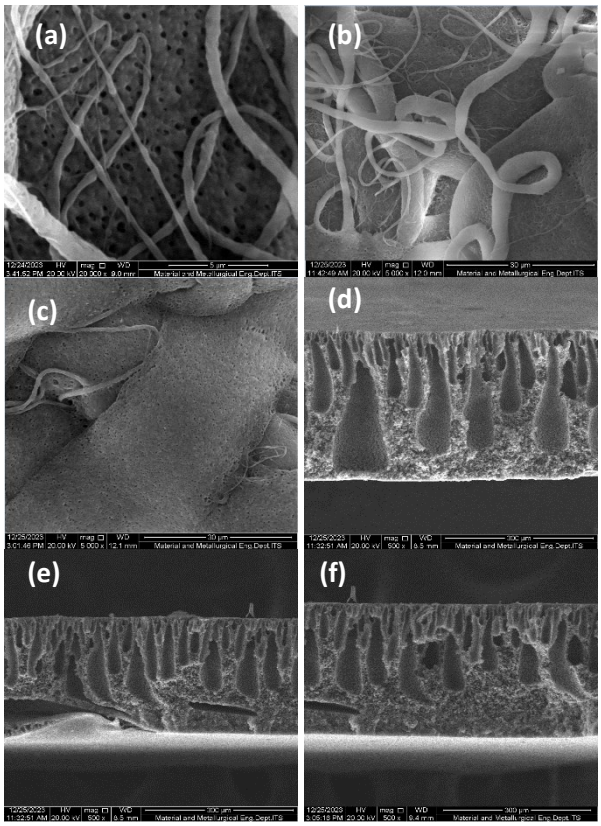

Fig. 2. SEM results of QGO-PVDF membrane surface and cross-section morphology: (a) Q0 surface, (b) Q3 surface, (c) Q5 surface, (d) Q0 cross-section, (e) Q3 cross-section, (f) Q5 cross-section

This was also supported by Young's modulus results as presented in Table 2 showing an increase in Young's modulus values with increasing QGO mass. The strong interactions between QGO particles allowed the formation of particle agglomerates, thereby reducing the gaps and voids (pores) between QGO particles. The decrease in pore sizes restricted the mobility of PVDF molecular chains. The PVDF molecular chains became less capable of crossing each other due to the densely packed QGO particles acting as barriers. As a result, the QGO-PVDF membranes became stiffer and harder with increasing QGO mass. The stiffness and hardness of the material were reflected in its Young's modulus value. The greater the Young's modulus of a substance, the higher its stiffness and hardness. Consequently, the findings of this investigation suggested that the rise in QGO mass resulting in augmented pore density in the QGO-PVDF membranes correlated directly with the elevation in Young's modulus values. The two were interrelated and signified the improved rigidity and hardness of the material.

According to the data on Young's modulus and AFM imaging, the Q5 membrane displayed an optimal overall performance. This membrane exhibited smaller pore dimensions and a more intricate porous configuration compared to the PVDF membrane (Q0), as evidenced in Fig. 5 and 6. Consequently, the Q5 membrane demonstrated enhanced surface roughness versus the Q0 membrane.

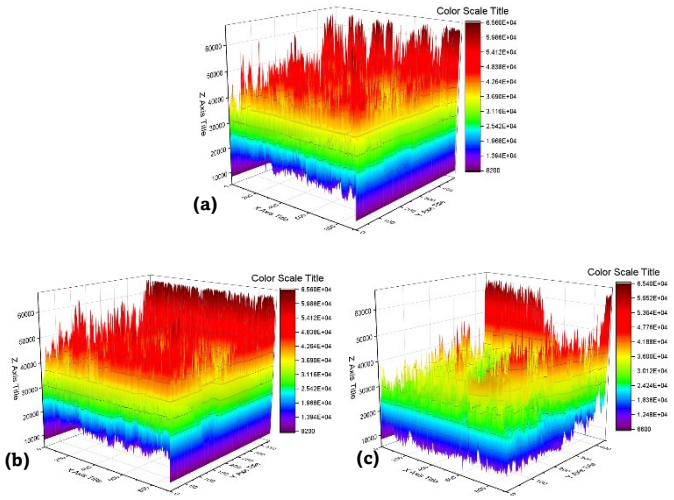

Fig. 3. 3D graph of QGO-PVDF membrane porosity: (a) Q0, (b) Q3, (c) Q5

While SEM images revealed the existence of pores in the QGO-PVDF membrane, and the SEM apparatus was unable to quantify the precise percentage of porosity within the membrane. Hence, this study employed OriginPro 2018 software to further determine the membrane's porosity using the SEM images. The origin software utilized physical formulae to calculate the porosity percentage and average sample size. The origin application yielded values for H max, H min, X, Y, and integral volume on solid polymer electrolyte samples [18,19]. These values were then used to compute the total volume, solid volume, the volume under the curve, pore volume, and the membrane porosity percentage. OriginPro 2018 software generated a 3D graph of the membrane porosity (Fig. 3) with the QGO-PVDF membrane porosity values as presented in Table 3.

Table.3 Porosity of QGO-PVDF Membrane

Membrane	PVDF (gram)	QGO (gram)	Porosity (%)
Q0	2.7	0	66.91
Q3	2.7	0.03	72.13
Q5	2.7	0.05	74.72

3.4. Membrane surface roughness analysis

Fig. 4 and 5 provide the insights of the AFM images into the three-dimensional (3D) morphology and surface roughness of the membranes. Notably, the QO (PVDF) and Q5 samples exhibited the distinct forms of peaks and depressions on their modified surfaces. The inclusion of inorganic nanoparticles in the organic polymer casting solution heightened the thermodynamic instability of the solution, resulting in the formation of rugged valleys during the casting solution's phase transition [29]. The results showed that the pure PVDF membrane (Q0) exhibited the smoothest surface with an average roughness (Ra) measuring 62.4 nm and a root mean square roughness (Rq) measuring 77.6 nm. In contrast, Q5 showed a significant increase in surface roughness with Ra measuring at 85.3 nm and Rq at 101.2 nm, compared to Q0. This increase in surface roughness was presumed to enlarge the surface area, thereby boosting the membrane flux, as demonstrated by the higher permeability values of pure water and Cu^{2+} solution on Q5 over Q0. Hence, it can be inferred that altering the composition of PVDF membranes may serve as a viable approach to improve membrane performance, especially regarding surface roughness and flux rate. This aligns with the discoveries made by Zhang et al. [30].

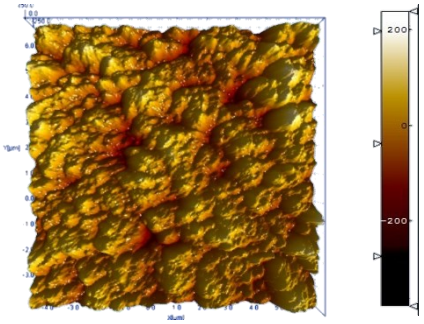

Fig. 4. The surface roughness of Q0

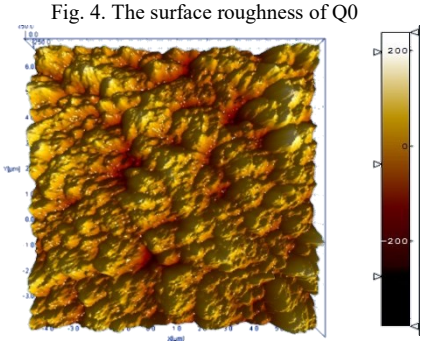

Fig. 5. The surface roughness of Q5

3.5. Evaluation of antibacterial properties of membrane

It is widely recognized that quaternary ammonium salts

possess a high density of positive charges and robust electrostatic interactions with the negatively charged membranes of bacterial cells. These compounds can penetrate bacterial cells via their alkyl chains, leading to bacterial inactivation [31]. To assess the antibacterial efficacy of both blank PVDF membranes and QGO-PVDF membranes, the disc diffusion method was employed. As depicted in Fig. 6, numerous bacterial colonies proliferated on the surface of blank PVDF membranes, whereas the QGO membranes exhibited considerably fewer colonies. The incorporation of QGO into the membranes resulted in the inhibition of bacterial colony growth. Notably, no distinct inhibition zone was observed around the QGO membranes, suggesting that the spread of bacteriostatic agents emitted by the membranes was limited. The presence of a larger inhibition zone typically indicated the loss of more readily diffusible antibacterial substances. As a carrier for quaternary ammonium salts, GO could be incorporated within the PVDF polymer membrane structure due to its irregular structure and hydrophobic carbon composition, thereby reducing the loss of QGO from the membrane surface.

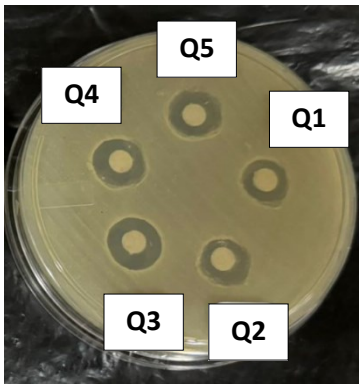

Fig. 6. Inhibitory zone of QGO-PVDF membrane

As indicated in Table 4, the incorporation of QGO into QGO-PVDF membranes resulted in a rise in antibacterial efficacy, corresponding to the escalating proportion of QGO utilized in the composition. It was indicated by the results of antibacterial activity testing using the disc diffusion method, where the higher the composition of QGO in the membrane, the wider the bacterial growth inhibition zone (inhibitory zone) generated. The addition of quaternary ammonium groups through QGO could provide more antibacterial agents that could bind and penetrate the bacterial cell membrane, thereby inhibiting metabolism and growth. The primary mechanism believed to enhance the antibacterial effectiveness of the QGO-PVDF membrane was attributed to the robust electrostatic interaction among the positive charged groups on QGO and the negative charged surface of bacterial cells.

Table 4. Antibacterial activity of QGO-PVDF membrane against E. coli

Membrane	PVDF (gram)	QGO (gram)	Inhibitory Zone (mm)
Q0	2.7	0	8.40
Q1	2.7	0.01	13.93
Q2	2.7	0.02	14.65
Q3	2.7	0.03	15.32
Q4	2.7	0.04	15.45
Q5	2.7	0.05	15.62

3.6. Water permeability test

Fig. 7 shows that the pure water flow via the PVDF membrane (Q0) was 756.33 $Lm^{-2}h^{-1}$. The flux values with the addition of QGO to the membrane were 805.2, 898.82, 1012.91, 1112.05, and 1208.25 $Lm^{-2}h^{-1}$ for membranes Q1, Q2, Q3, Q4, and Q5 respectively. The rise in flux was credited to the augmentation of hydrophilic groups: hydroxyl groups and quaternary ammonium, on the membrane surface owing to the inclusion of QGO. These hydrophilic functional groups attracted water molecules to the membrane surface, thereby facilitating their permeation through the membrane [25, 32]. In addition, membrane surface analysis using AFM characterization (Fig. 4, 5) showed a significant increase in surface roughness between Q0 and Q5. It was recognized that augmenting surface roughness could enlarge the effective filtration surface area of the membrane, thus aiding in the enhancement of membrane flux [25]. In summary, changes in water flux are associated with several factors, including hydrophilicity, surface roughness, pore dimensions, and porosity of the membrane. Therefore, changes in water flux are the result of a combination of these aspects.

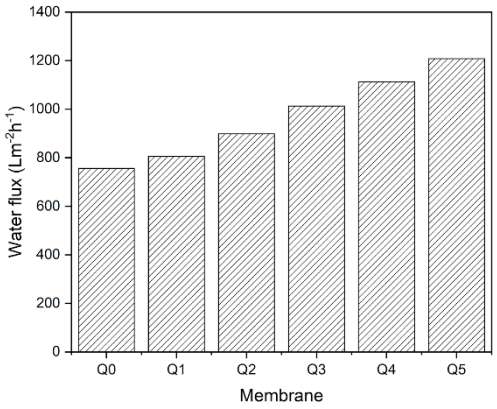

Fig. 7. Water permeation of the membranes

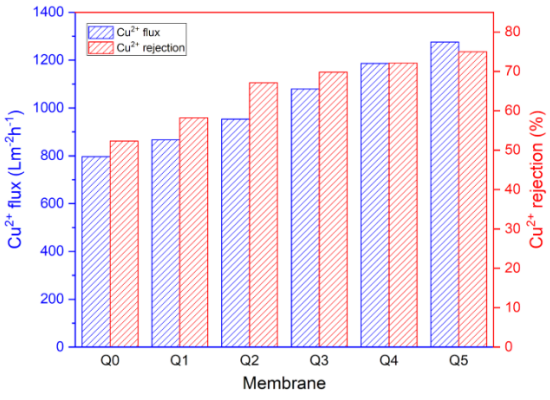

Fig. 8. Cu^{2+} flux and rejection of the membranes

3.7. Membrane flux and rejection properties test

The QGO-PVDF membrane's permeability and selectivity towards Cu^{2+} were assessed using a CuSO4 solution. The gradual addition of QGO mass increased both flux and rejection, as depicted in Fig. 4. The Cu^{2+} membrane filtration flux exhibited a rise from 796.74 to 1275.4 $Lm^{-2}h^{-1}$ with the

incremental addition of QGO mass from Q0 to Q5. This escalation was mainly ascribed to the increased abundance of quaternary hydroxyl and ammonium groups, which results in improved hydrophilic characteristics. The hydrophilic functional groups attract Cu^{2+} ions, facilitating the passage of the solution through the membrane [33]. Specifically, membranes with QGO addition (Q1-Q5) demonstrated flux values 8.8-60% higher than pure PVDF membrane (Q0). The superior performance can be attributed to the presence of QGO. Simultaneously, the addition of QGO led to an increase in Cu^{2+} rejection from approximately 52.3% in pure PVDF (Q0) to 75% in Q5. This heightened selectivity was primarily due to the quaternary hydroxyl and ammonium groups on the surface of QGO, which chelated with Cu^{2+} and enhanced the removal efficiency compared to the Q0 membrane. The adsorption of Cu^{2+} onto QGO occurred through ion exchange and surface complexation, with surface complexation being the dominant mechanism [25,34].

4. Conclusion

Polyvinylidene fluoride (PVDF) membranes, when modified with quaternized graphene oxide (QGO), effectively act as modifiers, concurrently enhancing the water-attracting properties and antibacterial attributes of the membrane surface. While previous studies have proposed various methods for achieving dual-function hydrophilicity and antibacterial properties, many involve intricate post-membrane treatments such as zwitterion modification. In contrast, the blending method involving QGO, as outlined in this study, achieved membrane fabrication and dual-function surface alteration in a singular process, rendering it more practical and competitive for industrial applications. Additionally, the incorporation of QGO resulted in a significant improvement in the material's mechanical robustness and flux of the modified membrane. Furthermore, unlike many existing antibacterial modifiers, QGO exhibited minimal detachment from the membrane owing to its unique structure, ensuring the longevity of antibacterial properties in QGO-PVDF membranes for extended applications.

Acknowledgments

The authors extend their appreciation for the financial support provided by the Ministry of Education, Culture, Research, and Technology of the Republic of Indonesia.

Author Contributions: Contributions from A.K. include conceptualization, methodology, formal analysis, drafting the original manuscript, review, and validation. Contributions from N.K. include formal analysis, writing, review, and editing. Contributions from P.S. include writing, reviewing, editing, project administration, analysis, and data curation. Contributions from S.M. include writing, reviewing, editing, project administration, and validation. Contribution from S.A.C. include writing, investigation, resourcing, and reviewing. Contributions from N.Z. include writing, reviewing, editing, and project administration. All authors have reviewed and approved the final article manuscript.

Funding: provided by the Ministry of Education, Culture, Research and Technology of the Republic of Indonesia under contract number B/51238/UN38.III.1/LK.04.00/2023.

Conflicts of Interest: none

References

1. W. Raza, J. Lee, N. Raza, Y. Luo, K. Kim, dan J. Yang *Removal of phenolic compounds from industrial waste water based on membrane-based technologies*. Journal of Industrial and Engineering Chemistry. 71 (2019) 1-18a
2. E.I. El-Aswar, H. Ramadan, H. Elkik, dan A.G. Taha, A *comprehensive review on preparation, functionalization and recent applications of nanofiber membranes in wastewater treatment*. Journal of Environmental Management. 301 (2022).
3. E. Zolghadr, M.D. Firouzjaei, S.A. Aktij, A. Aghaei, E.K. Wujcik, M. Sadrzadeh, et al., *An ultrasonic-assisted rapid approach for sustainable fabrication of antibacterial and anti-biofouling membranes via metal-organic frameworks*. Materials Today Chemistry, 26 (2022).
4. S. Zhou, Y. Qu, B. Yang, Q. Zhang, J. Wang, Y. Lin, et al., *Bio-based tannic acid as a raw material for membrane surface modification*. Desalination. 555 (2023).
5. D. Zhang, P. Tang, G. Chen, Y. Su, J. Ye, M. Zhu, W. Tao, X. Ruan, et al., *Enhanced organic matter degradation in shale gas wastewater treatment using Biofilm-Membrane bioreactors with varied filler Types, Pre-ozonation, and filler ratios*. Separation and Purification Technology. 331 (2024).
6. N. Kusumawati, P. Setiarso, dan S. Muslim, *Polysulfone/polyvinylidene fluoride composite membrane: Effect of coating dope composition on membrane characteristics and performance*. Rasayan Journal of Chemistry. 11 (2018) 1034–1041.
7. D.A. Jadhav, S. Pandit, J.M. Sonawane, P.K. Gupta, R. Prasad, dan A.D. Chendake, *Effect of membrane biofouling on the performance of microbial electrochemical cells and mitigation strategies*. Bioresource Technology Reports. 15 (2021).
8. M.D. Firouzjaei, S.F. Seyedpour, S.A. Aktij, M. Giagnorio, N. Bazrafshan, A. Mollahosseini, et al., *Recent advances in functionalized polymer membranes for biofouling control and mitigation in forward osmosis*. Journal of Membrane Science. 596 (2020).
9. C. Wang, C. Mu, W. Lin, dan H. Xiao, *Functional-modified polyurethanes for rendering surfaces antimicrobial: An overview*. Advances in Colloid and Interface Science. 283 (2020).
10. B. Mishra, J. Ghosh, N.C. Dubey, dan B.P. Tripathi, *Designing Anti(-bio)fouling membranes with synergistic grafting of quaternized and zwitterionic polymers through surface initiated atom transfer radical polymerization*. Separation and Purification Technology. 328 (2024).
11. B. Mustafa, T. Mehmood, Z. Wang, A.G. Chofreh, A. Shen, B. Yang, J. Yuan, et al., *Next-generation graphene oxide additives composite membranes for emerging organic micropollutants removal: Separation, adsorption and degradation*. Chemosphere. 308 (2022).
12. M.S.K. Chowdury, Y.J. Cho, S.B. Park, dan Y. Park, *Nanohybrid graphene oxide membranes functionalized using 3-mercaptopropyl trimethoxysilane for proton exchange membrane fuel cells*. Journal of Membrane Science. 663 (2022).
13. H. Qu, L. Huang, Z. Han, Y. Wang, Z. Zhang, Y. Wang, et al., *A review of graphene-oxide/metal–organic framework composites materials: characteristics, preparation and applications*. Journal of Porous Materials. 28 (2021) 1837–1865.
14. H.T. Nguyen, T.L. Ho, A. Pratomo, N.A. Ilsan, T. Huang, C.H. Chen, dan

E.Y. Chuang, *Enzymatically triggered graphene oxide released from multifunctional carriers boosts anti-pathogenic properties for promising wound-healing applications*. Materials Science and Engineering C. 128 (2021).

15. Y. Mai, Z. Wang, Y. Zhou, G. Wang, J. Chen, Y. Lin, et al., *From disinfectants to antibiotics: Enhanced biosafety of quaternary ammonium compounds by chemical modification*. Journal of Hazardous Materials. 460 (2023).
16. S. Changkhamchom, P. Kunanupatham, K. Phasuksom, dan A. Sirivat, *Anion exchange membranes composed of quaternized polybenzimidazole and quaternized graphene oxide for glucose fuel cell*. International Journal of Hydrogen Energy. 46 (2021) 5642–5652.
17. N. Kusumawati, P. Setiarso, A.B. Santoso, S. Muslim, Q. A'yun, dan M.M. Putri, *Characterization of poly(vinylidene fluoride) nanofiber-based electrolyte and its application to dye-sensitized solar cell with natural dyes*. Indonesian Journal of Chemistry. 23 (2023) 113.
18. O. Bricoveanu, I.C. Marinas, dan P. Preda, *Determination of the average pore-size and porosity in collagen by image processing of SEM micrographs*. 2022 International Semiconductor Conference (CAS). (2022) 223-226.
19. R.F. Mushaddaq, A.A. Bama, Ramlan, dan T. Lestariningsih, *Elektrolit Polimer Padat dari Pencampuran PVDF-HFP dan PEO serta Modifikasi Filler Sebagai Bahan Dasar Baterai Lithium-Ion*. Jurnal Sains Dan Teknologi. 12 (2023) 219–228.
20. X. Xu, Q. Wang, X. Zhu, Q. Wu, T. Zheng, H. Yuan, dan Z. Zhou, *The preparation of anti-fouling dual-layer composite membrane with embedding graphene oxide*. Asia-Pacific Journal of Chemical Engineering. (5) (2023).
21. A. Islam, A.N. Khan, M.F. Shakir, dan K. Islam, *Strengthening of β polymorph in PVDF/FLG and PVDF/GO nanocomposites*. Materials Research Express. 7 (2020).
22. N. Kusumawati, P. Setiarso, S. Muslim, dan N. Purwidiani, *Synergistic Ability Of Psf And Pvdf To Develop High-Performance Psf/Pvdf Coated Membrane For Water Treatment*. Rasayan Journal of Chemistry. 11 (2018) 260-279.
23. T. Xue, W. Fan, X. Zhang, X. Zhao, F. Yang, dan T. Liu, *Layered double hydroxide/graphene oxide synergistically enhanced polyimide aerogels for thermal insulation and fire-retardancy*. Composites. Part B, Engineering. 219 (2021).
24. S. Song, S. Xia, Y. Wei, X. Lv, S. Sun, dan Q. Li, *Fluoro-polymer-coated carbon nanotubes for improved interfacial interactions and dielectric properties in MWCNTs/PVDF composites*. Journal of Materials Science. 55 (2020) 3212–3227.
25. R.H. Alasfar, S. Ahzi, N. Barth, V. Kochkodan, M. Khraisheh, dan M. Koç *A review on the modeling of the elastic modulus and yield stress of polymers and polymer nanocomposites: Effect of temperature, loading rate and porosity*. Polymers. 14 (2022) 360.
26. H. Essabir, M. Raji, R. Rodrigue, R. Bouhfid, A.K. Qaiss, *Multifunctional poly (vinylidene fluoride) and styrene butadiene rubber blend magneto-responsive nanocomposites based on hybrid graphene oxide and Fe 3 O 4: synthesis, preparation and characterization*. Journal of Polymer Research. 28 (2021) 1-17.
27. H. Liu, X. Liu, F. Zhao, Y. Liu, L. Liu, L. Wang, et al., *Preparation of a hydrophilic and antibacterial dual function ultrafiltration membrane with quaternized graphene oxide as a modifier*. Journal of Colloid and Interface Science. 562 (2020) 182–192.
28. G. Zhao, R. Hu, X. Zhao, Y. He, dan H. Zhu, *High flux nanofiltration membranes prepared with a graphene oxide homo-structure*. Journal of Membrane Science. 585 (2019) 29-37.
29. X. Tan, dan D. Rodrigue, *A review on porous polymeric membrane preparation. Part I: Production techniques with polysulfone and poly (vinylidene fluoride). Polymers. 11 (2019)..*
30. X. Zhang, Y. Zhou, F. Zhao, C. Geng, Z. Li, J. Zhang, et al., *Anti-fouling mechanism of ultrafiltration membranes modified by graphene oxide with different charged groups under simulated seawater conditions*. Journal of Membrane Science. 674 (2023).
31. J. Jiang, Y. Zou, Q. Sun, S. Liu, M. Sun, H. Zheng, dan H. Li, *Copolymers functionalized with quaternary ammonium compounds under template chain exhibit simultaneously efficient bactericidal and flocculation properties: Characterization, performance and mechanism*. Journal of Hazardous Materials, 465 (2024)
32. Y. Li, S. Huang, S. Zhou, A.G. Fane, Y. Zhang, dan S. Zhao, *Enhancing water permeability and fouling resistance of polyvinylidene fluoride membranes with carboxylated nanodiamonds*. Journal of Membrane Science. 556 (2018) 154–163.
33. Y. Liu, Y. Zhao, X. Wang, X. Wen, X. Huang, dan Y.F. Xie, *Effect of varying piperazine concentration and post-modification on prepared nanofiltration membranes in selectively rejecting organic micropollutants and salts*. Journal of Membrane Science. 582 (2019) 274–283.
34. H. Awes, Z. Zaki, S. Abbas, H. Dessoukii, A. Zaher, S.A. Abd-El Moaty, et al., *Removal of Cu^{2+} metal ions from water using Mg-Fe layered double hydroxide and Mg-Fe LDH/5-(3-nitrophenyllazo)-6-aminouracil nanocomposite for enhancing adsorption properties*. Environmental Science and Pollution Research International. 28 (2019) 47651–47667.